IOP Publishing Semiconductor Science and Technology
Semicond. Sci. Technol. **31** (2016) 075001 (6pp) doi:10.1088/0268-1242/31/7/075001

Noise temperature in graphene at high frequencies

Raúl Rengel, José M Iglesias, Elena Pascual and María J Martín

Department of Applied Physics, University of Salamanca, Salamanca 37008, Spain

E-mail: raulr@usal.es

Received 7 March 2016, revised 26 April 2016
Accepted for publication 5 May 2016
Published 24 May 2016

Abstract

A numerical method for obtaining the frequency-dependent noise temperature in monolayer graphene is presented. From the mobility and diffusion coefficient values provided by Monte Carlo simulation, the noise temperature in graphene is studied up to the THz range, considering also the influence of different substrate types. The influence of the applied electric field is investigated: the noise temperature is found to increase with the applied field, dropping down at high frequencies (in the sub-THz range). The results show that the low-frequency value of the noise temperature in graphene on a substrate tends to be reduced as compared to the case of suspended graphene due to the important effect of remote polar phonon interactions, thus indicating a reduced emitted noise power; however, at very high frequencies the influence of the substrate tends to be significantly reduced, and the differences between the suspended and on-substrate cases tend to be minimized. The values obtained are comparable to those observed in GaAs and semiconductor nitrides.

Keywords: Monte Carlo, noise, graphene, high frequency

(Some figures may appear in colour only in the online journal)

1. Introduction

Since its experimental demonstration in 2004 [1], the interest in the use of graphene as the base material for future electronics and potential replacement of traditional semiconductors has risen exponentially. The most promising applications are those in which the absence of a bandgap is not a drawback, so the devices can benefit from the excellent electronic transport properties of this material [2]. In particular, graphene field effect transistors (GFETs) have been proposed as very appealing candidates for developing new devices aimed for high frequency analog applications [3, 4]. Cut-off frequencies have been reported for experimental devices over 300 and 427 GHz, with values reaching the THz range projected by static measurements and simulations [5–8]. However, in this context the feasibility of GFETs for future developments of analog graphene technology will be determined not only by their operating frequencies, but especially for the noise properties of this material and its influence on device performance. Low-frequency noise has been studied by several authors in monolayer graphene [9, 10] and GFETs [11–13]. Recently, the influence of the substrate on the $1/f$ noise in a GFET has also been shown, evidencing low-frequency noise suppression in the case of graphene on a substrate [14]. Regarding high-frequency noise performance, some recent studies have dealt with this subject in graphene devices (see, e.g. [15–17]). In the microwave frequency range (a usual range for amplifiers) thermal noise is dominant in GFETs [17]. Within this context, it becomes imperative to acquire a deep understanding of the noise properties in graphene at the material level, with particular focus on the investigation of thermal noise processes at high frequencies. In order to characterize the thermal noise behavior, the noise temperature [18] T_n is an important parameter both from an experimental and modeling point of view, applied also to the particular case of GFETs [17, 19]. While in a GFET a unique noise temperature for the whole device is usually considered, a method for determining the frequency and electric field dependence of this figure of merit in monolayer graphene is very appealing not only to achieve a better understanding of electronic noise processes in graphene, but also in the context of device noise modeling, since T_n can be related to the local noise sources in the channel in a straightforward manner. In this way, a link can be established between the local noise

sources and the macroscopic noise performance of the devices. Noise temperature has been extensively investigated in traditional semiconductors at the material level, e.g. in Si, GaAs, GaN, InN, etc [20–22]. In these cases, the importance of a deep understanding of the differential mobility, power spectral density of current fluctuations (diffusion coefficient) and noise temperature (and their spectra) has been shown, in order to elucidate the noise behavior of the materials in the high-frequency regime. Numerical simulation tools, in particular the Monte Carlo method [23], have proved their suitability to achieve this goal. In the case of graphene, such study remains unexplored.

In this work, we present a rigorous microscopic approach, based on an ensemble Monte Carlo (EMC) simulator, that allows one to determine the noise temperature (including its frequency dependence) in the particular case of graphene. The method also involves calculating the differential mobility and the power spectral density of velocity fluctuations (that provides the diffusion coefficient); the influence of different substrate types is also taken into account. In section 2.1 the noise temperature in the specific case of graphene is thoroughly determined, attending to the specific properties of the linear dispersion relation in this material. The main features of the Monte Carlo procedure are described in section 2.2. The results and discussion are presented in section 3. Finally, the main conclusions are drawn.

2. Theoretical background and modelling procedure

2.1. The noise temperature

Let us consider a graphene sheet with dimensions W (in the y direction) and L (in the x direction) and a carrier density equal to n, with two contacts at the ends (i.e., $x = 0$ and $x = L$). In a general case, the power spectral density of the current fluctuations generated by a single carrier can be obtained as [24]:

$$S_{\Delta i}(f) = \frac{q^2}{L^2} S_{\Delta v_x}(f) = 4\frac{q^2}{L^2} D(f) \tag{1}$$

$S_{\Delta v_x}$ being the power spectral density of velocity fluctuations, that is related to the diffusion coefficient coefficient $D(f)$ through the Wiener–Kintchine theorem [23], and q being the electron charge. The total number of carriers in the sample is $N = nWL$. In the case of non-degenerate systems, the contributions of these carriers to the total current $I(t)$ and to its power spectral density $S_{\Delta I}(f)$ are independent [24], and therefore:

$$S_{\Delta I}(f) = N S_{\Delta i}(f) = nWL S_{\Delta i}(f) = 4\frac{q^2 nW}{L} D(f) \tag{2}$$

However, in the case of graphene we must consider a degenerate system. This implies that the electrons are no longer independent, and the second member of equation (2) must be multiplied by the ratio $\Delta\bar{N}^2/\bar{N}$, where $\Delta\bar{N}^2$ is the variance of the number of carriers and $\bar{N}$ is the average total number. From statistical mechanics, [24, 25] this ratio can be expressed as:

$$\frac{\Delta\bar{N}^2}{\bar{N}} = \frac{k_B T}{n}\left(\frac{\partial n}{\partial \varepsilon_F}\right) \tag{3}$$

ε_F being the Fermi level, k_B the Boltzmann constant and T the system temperature. Considering the energy dependent density of states $g(\varepsilon)$ in graphene [26] and defining $\eta = \varepsilon/k_B T$ it is possible to obtain:

$$n = \frac{2}{\pi}\left(\frac{k_B T}{\hbar v_F}\right)^2 \int_0^\infty \frac{\eta}{1 + e^{(\eta - \eta_F)}}\, d\eta \tag{4}$$

From this expression, in the case of graphene we get:

$$\frac{\Delta\bar{N}^2}{\bar{N}} = \frac{\int_0^\infty \eta \frac{e^{(\eta-\eta_F)}}{(1+e^{(\eta-\eta_F)})^2}\, d\eta}{\int_0^\infty \frac{\eta}{1+e^{(\eta-\eta_F)}}\, d\eta} \tag{5}$$

Therefore, getting back to equation (2) and multiplying by this degeneracy factor we have:

$$S_{\Delta I}(f) = 4\frac{q^2 nW}{L} D(f) \frac{\int_0^\infty \eta \frac{e^{(\eta-\eta_F)}}{(1+e^{(\eta-\eta_F)})^2}\, d\eta}{\int_0^\infty \frac{\eta}{1+e^{(\eta-\eta_F)}}\, d\eta} \tag{6}$$

On the other hand, the power spectral density of current fluctuations can be obtained as [24, 27]:

$$S_{\Delta I}(f) = 4k_B T_n(f) \mathrm{Re}[Y(f)] p(f) \tag{7}$$

where $\mathrm{Re}[Y(f)]$ is the real part of the complex admittance, that is equal to $qnW\mu(f)/L$ (with $\mu(f)$ being the real part of the differential mobility), T_n is the noise temperature [27] and $p(f)$ is the quantum correction factor for thermal noise, i.e. [24]:

$$p(f) = \frac{hf/2k_B T}{\tanh(hf/2k_B T)} \tag{8}$$

The frequency-dependent generalized Einstein relation in graphene is obtained by comparing equations (6) and (7), and consequently the frequency dependent noise temperature in graphene can be defined as:

$$T_n(f) = \frac{qD(f)}{k_B \mu(f) p(f)} \frac{\int_0^\infty \eta \frac{e^{(\eta-\eta_F)}}{(1+e^{(\eta-\eta_F)})^2}\, d\eta}{\int_0^\infty \frac{\eta}{1+e^{(\eta-\eta_F)}}\, d\eta} \tag{9}$$

This frequency dependent noise temperature is related to the maximum fluctuating power per unit bandwidth displayed to an output circuit [20]. Consequently, it provides additional information about the high-frequency performance, since it is the combination of the noise (velocity fluctuations) and dynamic (mobility or equivalently, conductivity) properties of the system [20].

2.2. Monte Carlo procedure

In this work, the frequency dependent mobility and diffusion coefficient are computed by means of an in-house ensemble Monte Carlo (EMC) simulator, whose main features are described in [28, 29]. Each quantity is calculated using a separate procedure. The calculation of the diffusion coefficient is carried out by means of the Fourier analysis of instantaneous velocity fluctuations, that provides their power spectral density, considering background and excess populations coupled by a exchange carrier-carrier mechanism, as described in [30]. We successfully applied this methodology to the case of suspended graphene and graphene on a substrate [28, 29], finding that intrinsic optical phonons and remote polar phonons play a significant role in determining this quantity.

The frequency dependent differential mobility is computed in the time domain by analyzing the evolution of two separate halves of the excess carrier ensemble conveniently perturbed, following the methodology described in [31] and applied here to the case of graphene:

$$\mu(f) = \int_0^\infty K_v(t) \mathrm{e}^{-i2\pi ft} \mathrm{d}t \tag{10}$$

with K_v being the response function relating the perturbation of the field and the modulation of the drift velocity. This function is obtained by dividing the particle ensemble into two halves, P and M. At a given time, particles in the P set increase their individual momentum p_i by a small amount δp, and carriers in the M set decrease it by the same amount. Then, the system is allowed to return to the stationary condition and the time evolution of the average velocities of each half is recorded, so K_v can be obtained as [31]:

$$K_v(t) = (q/2\delta p)(\langle v_i \rangle_P - \langle v_i \rangle_M) \tag{11}$$

The simulator includes interactions with intrinsic acoustic intravalley phonons, in-plane TO and LO branches for optical phonons and TA and LA for acoustic intervalley phonons, with the deformation potential parameters provided by first-principles calculations [32]. Out-of-plane optical and acoustic branches are much smaller than in-plane ones, at least 3 orders of magnitude [32], so its influence can be regarded as negligible in the applied field range considered. The influence of surface polar phonons is also taken into account by considering the associated anisotropic inelastic scattering mechanism. This is obtained by including the Fröhlich coupling, the screening function and the van der Waals distance between the polar substrate and the graphene flake, as described in [33–36]. The parameters considered for the different substrate types are shown in [29]. SiO_2 substrate has been considered, as in most practical situations. The case of graphene on h-BN and suspended graphene are studied also for comparison. The number of particles considered in the simulation ranges from 10^5 to 2×10^6 depending on the parameter to be determined and the applied field and substrate material considered. The simulation is carried out in the reciprocal space, and the graphene sheet is considered to be large enough so edge effects or modifications of the band structure due to small dimensions (as in nanoribbons) are negligible.

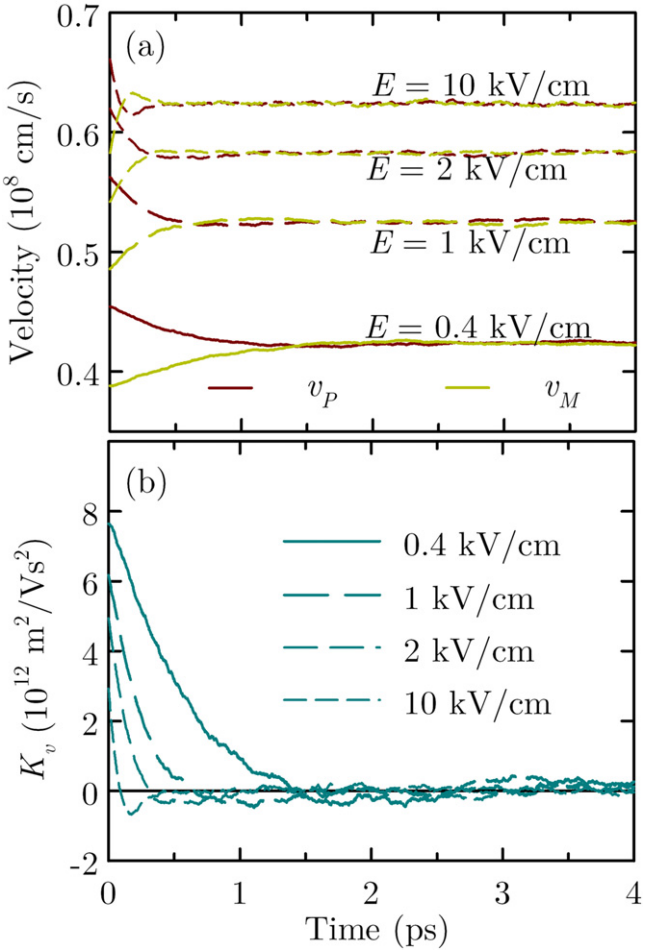

Figure 1. Instantaneous average velocity of carriers in the P and M ensembles for several values of the electric field, 0.4, 1, 2 and 10 kV/cm (a). Response function K_v as a function of time (b). The graphene layer is placed on top of a SiO_2 substrate.

3. Results and discussion

Figure 1(a) shows the evolution of the average velocities of the P and M sets for graphene on SiO_2 for several different values of the applied field (0.4, 1, 2 and 10 kV/cm) and a carrier concentration equal to 10^{12} cm^{-2} when a small perturbation of the electron momentum is applied. As can be observed, for those applied fields the system tends to return to the stationary situation very quickly; with a shorter transient the higher the field. Moreover, we observe a small velocity crossover at 2 ps for 0.4 kV/cm, 1 ps for 1 kV/cm, 0.5 ps for 2 kV/cm and 0.2 ps for 10 kV/cm, with the M set showing larger velocities than the P set for a short time. This crossover is responsible for a negative value of the linear response coefficient K_v, as shown in figure 1(b).

The frequency-dependent differential mobility for graphene on SiO_2 is shown in figure 2. The real part presents a flat dependence at low frequencies extending to different

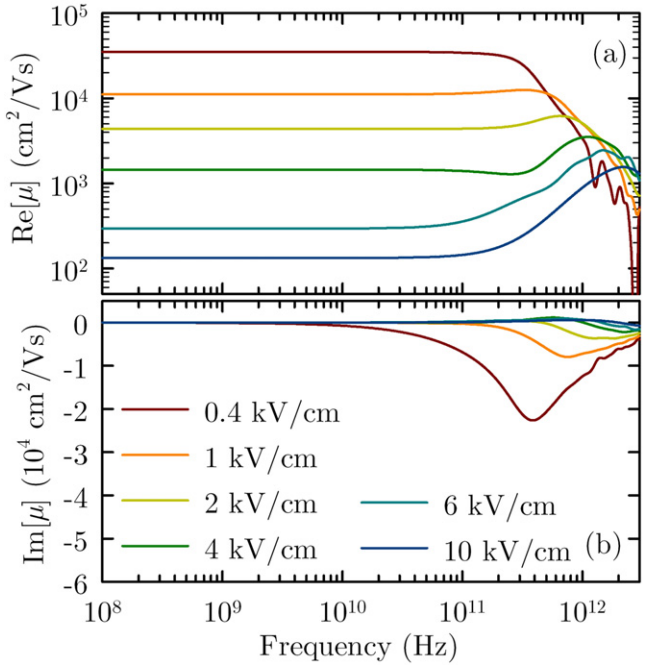

Figure 2. Real (a) and imaginary (b) parts of the differential mobility as a function of frequency, for several electric fields applied, in graphene on SiO_2.

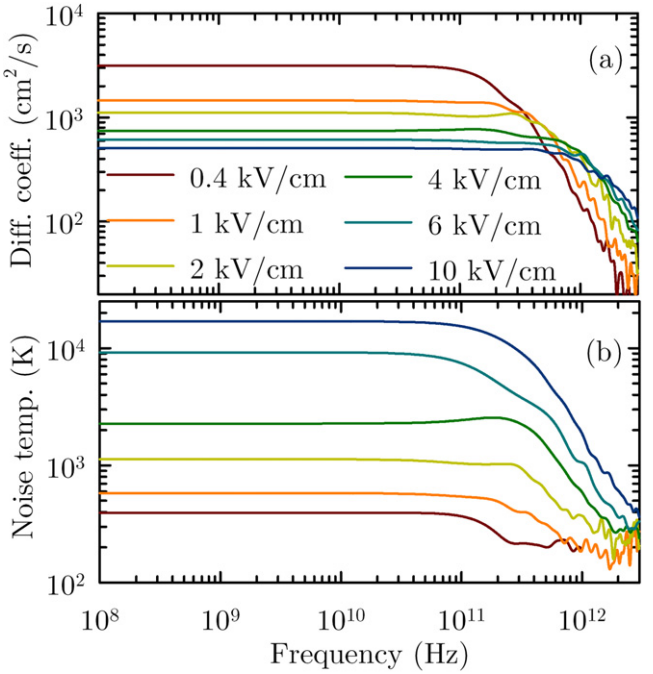

Figure 3. Diffusion coefficient (a) and noise temperature (b) as a function of frequency for several electric fields applied, in graphene on SiO_2.

spectra depending on the electric field applied. At low fields, it shows a Lorentzian shape, with the constant low-frequency mobility kept up to the THz range, while as the electric field increases this flat region is maintained up to smaller frequencies. At high fields a bump appears; it becomes more pronounced and happens at larger frequencies as the field is increased. This bump is related to a comparatively larger negative part of the K_v, that appears at very short times and is related to the decoupling of velocity and energy relaxation processes [20, 21]. The imaginary part (which is related to a reactive contribution to the material conductance [21]) shows negligible values at low frequencies, and then it presents a maximum at very high frequencies for low applied fields, corresponding to the corner frequency for the real part. This behavior is consistent with recent experimental measurements in graphene, in which the imaginary part of the conductivity shows a Drude–Smith dependence with the frequency [37].

The diffusion coefficient (that is directly obtained from the power spectral density of velocity fluctuations) is presented in figure 3(a). It shows a Lorentzian shape, with the low-frequency value being reduced as the applied field is increased and the corner frequency reaching higher frequencies for high fields. This larger corner frequency is due to a faster break of the velocity correlation at high field as a consequence of a larger amount of scattering events, particularly for optical phonons and remote polar phonons from the substrate [29]. Once that the frequency-dependent mobility and diffusion coefficient are determined, the noise temperature is directly obtained from equation (9). The results are shown in figure 3(b). There is a monotonic trend for the noise temperature to increase as the electric field is raised, a consequence of a larger noise intensity provoked by a more pronounced scattering activity. At the lower field value the low-frequency noise temperature is close to the equilibrium value (290 K), and then it significantly raises even over 10^4 K. On the other hand, at high frequencies the noise temperature tends to reduce: this reduction is driven by the drop in the diffusivity. This noise temperature spectrum is similar to those observed in Si, GaAs and semiconductor nitrides [20–22]. This curved shape cannot be interpreted in terms of a single Lorentzian based on physical parameters; the noise temperature in traditional semiconductors has shown similar Lorentzian shapes that have been interpreted in terms of complex analytical expressions derived from a linearized Boltzmann equation [20, 21] that do not correspond to single Lorentzians.

Finally, we have evaluated the impact of the substrate type on the noise temperature. Figure 4 shows the low-frequency value of the noise temperature as a function of the applied electric field for three different cases: graphene on SiO_2, graphene on h-BN and suspended graphene. As can be seen, at low applied fields the noise temperature tends to be close to the equilibrium value (290 K) in all cases, and then it is significantly raised as the electric field is increased and the average energy of the electron system is augmented. The results are in the same order of magnitude as those observed in GaAs [20]. The increase of the noise temperature with the applied field is more intense in suspended graphene and, to a lesser extent, in graphene on h-BN, and in both cases it is larger than in graphene on SiO_2. This is provoked by a faster drop in the electron differential mobility, that is more evident in suspended graphene and graphene on h-BN due to a more pronounced negative differential conductivity in the velocity-field curves [29]. In the case of suspended graphene this drop

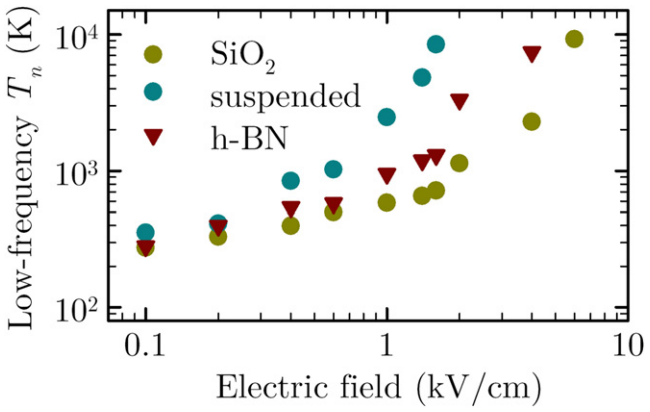

Figure 4. Low-frequency noise temperature as a function of the applied electric field for graphene on SiO_2, graphene on h-BN and suspended graphene.

in the differential mobility is related to a more intense optical phonon activity, that strongly reorients the electron wavevector and is translated into a reduction of the average velocity for a given applied field. In suspended graphene the electric field is much more efficient in increasing the average carrier energy, thus augmenting the optical phonon activity at a given electric field value. In the case of graphene on SiO_2, the important dominance of the remote polar phonon scattering, which is strongly anisotropic by nature, provokes a reduction in the average electron energy and a more effective orientation of the electron wavevector by the electric field, which leads to a less severe reduction of the differential mobility. In the case of graphene on h-BN the higher remote polar phonon energies appease the influence of this type of scattering, leading to an intermediate situation. At high fields, T_n would reach negative values due to the onset of negative differential mobility, and therefore it could not be defined according to equation (9), as in the case of III-V diodes [38]. In suspended graphene this condition is reached at lower fields than in graphene on substrates.

As it concerns the frequency dependence, figure 5(b) shows the spectrum of T_n for a given intermediate field (1 kV/cm), for which T_n can be defined in all cases. As can be observed, T_n starts dropping at lower frequencies in suspended graphene, and remains in a plateau at higher frequencies in graphene on SiO_2. This is due, on the one hand, to a minor corner frequency in the power spectral density of velocity fluctuations [29] (and hence, in the diffusivity), and, on the other hand, to the much larger comparative increase of the mobility with frequency in suspended graphene (figure 5(a)), which is due to a faster response of free carriers to a linear perturbation, providing negative values of the K_v function.

4. Conclusion

A numerical method for determining the frequency dependent noise temperature in graphene has been presented. The values obtained are comparable to those observed in GaAs and semiconductor nitrides. The results also indicate that there is

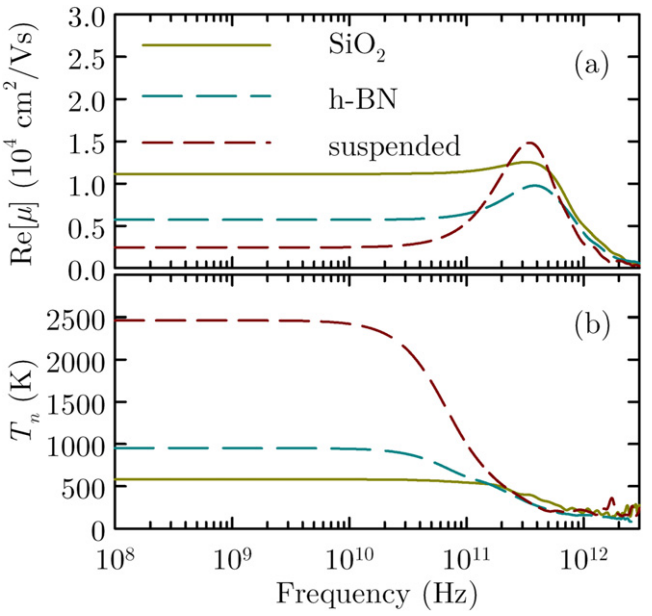

Figure 5. Real part of the differential mobility (a) and noise temperature (b) as a function of frequency for graphene on SiO_2, graphene on h-BN and suspended graphene. The applied electric field is 1 kV/cm.

an important influence of remote polar phonons in determining both the low-frequency noise temperature and also its frequency spectrum. Since the noise temperature is directly related to the output power emitted by a sample due to the stochastic electromagnetic radiation produced by the scattering interactions and accelerating electric fields suffered by single carriers [21], it can be concluded that in the case of graphene on SiO_2 the emitted noise power at low frequencies is noticeably reduced as compared to the case of suspended graphene for a given electric field, while at high frequencies the differences with regard to suspended graphene and graphene on h-BN are significantly minimized.

Acknowledgments

This work was supported by research project TEC2013-42622-R from the Ministerio de Economía y Competitividad.

References

[1] Novoselov K S, Geim A K, Morozov S V, Jiang D, Zhang Y, Dubonos S V, Grigorieva I V and Firsov A A 2004 *Science* **306** 666–9
[2] Novoselov K S, Fal'ko V I, Colombo L, Gellert P R, Schwab M G and Kim K 2012 *Nature* **490** 192–200
[3] Schwierz F 2010 *Nat. Nanotechnol.* **5** 487–96 ISSN 1748-3387
[4] Yang X, Liu G, Rostami M, Balandin A and Mohanram K 2011 *IEEE Electron Device Lett.* **32** 1328–30
[5] Liao L, Lin Y C, Bao M, Cheng R, Bai J, Liu Y, Qu Y, Wang K L, Huang Y and Duan X 2010 *Nature* **467** 305–8
[6] Liao L, Bai J, Cheng R, Lin Y C, Jiang S, Qu Y, Huang Y and Duan X 2010 *Nano Letters* **10** 3952–6

[7] Cheng R, Bai J, Liao L, Zhou H, Chen Y, Liu L, Lin Y C, Jiang S, Huang Y and Duan X 2012 *Proc. Nat. Acad. Sci.* **109** 11588–92

[8] Zheng J, Wang L, Quhe R, Liu Q, Li H, Yu D, Mei W N, Shi J, Gao Z and Lu J 2013 *Sci. Rep.* **3** 1314

[9] Iannaccone G, Betti A and Fiori G 2011 Noise in graphene and carbon nanotube devices *21st Int. Conf. on Noise and Fluctuations (ICNF) (2011)* pp 360–3

[10] Pellegrini B 2013 *Eur. Phys. J.* B **86** 373

[11] Heller I, Chatoor S, Männik J, Zevenbergen M A G, Oostinga J B, Morpurgo A F, Dekker C and Lemay S G 2010 *Nano Lett.* **10** 1563–7 pMID: 20373788

[12] Zhang Y, Mendez E E and Du X 2011 *ACS Nano* **5** 8124–30 pMID: 21913642

[13] Moon J S *et al* 2011 *IEEE Electron Device Lett.* **32** 270–2 ISSN 0741-3106

[14] Stolyarov M A, Liu G, Rumyantsev S L, Shur M and Balandin A A 2015 *Appl. Phys. Lett.* **107** 023106

[15] Ardaravicius L, Liberis J, Sermuksnis E, Matulionis A, Hwang J, Kwak J Y, Campbell D, Alsalman H A, Eastman L F and Spencer M G 2013 *Physica Status Solidi (RRL) Rapid Res. Lett.* **7** 348–51

[16] Mele D, Fregonese S, Lepilliet S, Pichonat E, Dambrine G and Happy H 2013 High frequency noise characterisation of graphene fet device *IEEE MTT-S Int. Microwave Symposium Digest (IMS) (2013)* pp 1–4

[17] Tanzid M, Andersson M A, Sun J and Stake J 2014 *Appl. Phys. Lett.* **104** 013502

[18] Pospieszalski M 1989 *IEEE Trans. Microw. Theory Tech.* **37** 1340–50

[19] Andersson M, Habibpour O, Vukusic J and Stake J 2012 Noise figure characterization of a subharmonic graphene fet mixer *Microwave Symposium Digest (MTT), IEEE MTT-S Int.* pp 1–3

[20] Varani L, Houlet P, Vaissière J C, Nougier J P, Starikov E, Gruzhinskis V, Shiktorov P, Reggiani L and Hlou L 1996 *J. Appl. Phys.* **80** 5067–75

[21] Reggiani L, Starikov E, Shiktorov P, Gruzinskis V and Varani L 1997 *Semicond. Sci. Technol.* **12** 141

[22] Starikov E, Shiktorov P, Gruinskis V, Varani L, Vaissière J C, Palermo C and Reggiani L 2005 *J. Appl. Phys.* **98** 083701

[23] Jacoboni C and Lugli P 1989 *The Monte-Carlo Method for Semiconductor Device Simulation* (Wien: Springer) ISBN 9783211821107

[24] van Vliet K and van der Ziel A 1977 *Solid-State Electron.* **20** 931–3

[25] Landau L and Lifshitz E 1996 *Statistical Physics* (Oxford: Elsevier Science) v.5 ISBN 9780080570464

[26] Wong H S P and Akinwande D 2011 *Carbon Nanotube and Graphene Device Physics* 1st edn (Cambridge, UK: Cambridge University Press)

[27] Nougier J P 1994 *IEEE Trans. Electron Devices* **41** 2034–49

[28] Rengel R and Martín M J 2013 *J. Appl. Phys.* **114** 143702

[29] Rengel R, Pascual E and Martín M J 2014 *Appl. Phys. Lett.* **104** 233107

[30] Thobel J L, Sleiman A and Fauquembergue R 1997 *J. Appl. Phys.* **82** 1220–6

[31] Price P J 1983 *J. Appl. Phys.* **54** 3616–17

[32] Borysenko K M, Mullen J T, Barry E A, Paul S, Semenov Y G, Zavada J M, Nardelli M B and Kim K W 2010 *Phys. Rev.* B **81** 121412

[33] Fratini S and Guinea F 2008 *Phys. Rev.* B **77** 195415

[34] Perebeinos V and Avouris P 2010 *Phys. Rev.* B **81** 195442

[35] Konar A, Fang T and Jena D 2010 *Phys. Rev.* B **82** 115452

[36] Li X, Barry E A, Zavada J M, Nardelli M B and Kim K W 2010 *Appl. Phys. Lett.* **97** 232105

[37] Buron J D, Pizzocchero F, Jepsen P U, Petersen D H, Caridad J M, Jessen B S, Booth T J and Bøggild P 2015 *Sci. Rep.* **5** 12305

[38] Shiktorov P, Gružinskis V, Starikov E, Reggiani L and Varani L 1996 *Phys. Rev.* B **54** 8821–32